Observation of Transonic Ionization Fronts in Low-Density Foam Targets

D. Hoarty,[1,2] L. Barringer,[1] C. Vickers,[1] O. Willi,[1] and W. Nazarov[3]
[1]*Imperial College of Science, Technology and Medicine, London, United Kingdom*
[2]*Radiation Physics Department, AWE Aldermaston, Reading, Berkshire, United Kingdom*
[3]*Chemistry Department, University of Dundee, United Kingdom*
(Received 13 July 1998)

Transonic ionization fronts have been observed in low-density chlorinated foam targets using time-resolved K-shell absorption spectroscopy. The front was driven by an intense pulse of soft x rays produced by high-power laser irradiation of a thin foil. The density and temperature profiles inferred from the radiographs provided detailed measurement of the conditions at a number of times. The experimental data were compared to radiation hydrodynamics simulations and reasonable agreement was obtained. [S0031-9007(99)08879-1]

PACS numbers: 52.50.Jm, 47.70.Mc, 52.25.Nr

The study of the interaction of intense radiation with low density matter has applications in astrophysics—for example, in the understanding of radiative flow in stellar envelopes and interstellar material [1], in the initiation of stellar gravitational collapse, and in inertial confinement fusion research [2]. An intense radiation flux rapidly ionizes and heats the low-density material which, when heated, has a small opacity to incident radiation. Radiation thus passes through the heated material and is absorbed at the boundary of the cold material, creating a front which propagates as an ionization wave. The ionization wave may propagate supersonically or be preceded by a shock. Supersonic propagation of radiatively driven fronts has been observed in low density foams [3] and subsonic propagation has been seen in x-ray driven foils [4]. Ionization fronts propagating through material supersonically may eventually relax to a subsonic front. The gas dynamics of low-density material heated by intense radiation has been described by several workers [5,6]. Analytic solutions to the propagation of heat and ionization fronts have been derived for steady supersonic and subsonic fronts preceded by a strong shock but not for the transonic behavior between the two regimes. Conditions in the transonic regime are uncertain due to their sensitivity to the radiative opacity of the plasma behind the front, the emission from the ionization front, and hydrodynamic effects influencing the pressure in the hot, ionized material. The calculation of the conditions in this transient phase is a complicated atomic physics and radiation hydrodynamics problem. Propagation of transonic ionization fronts has not been observed directly, though such fronts are known to occur in the corona of certain stars and in terrestrial plasmas. The use of low density foam to study ionization fronts has several advantages. Radiography can be carried out on extended targets in which supersonic propagation can be maintained for a time significantly longer than experimental time resolution and the transition to a subsonic ionization wave and ablative shock can be observed.

This Letter reports on the first direct observations of ionization fronts in the transonic regime using point projection spectroscopy [7]. The front was driven through a low density chlorinated foam target by an intense pulse of soft x-ray radiation [3,8]. The absorption spectrum of the chlorine doped into the foam enabled the temperature distribution in the foam to be inferred and the radiographs also provided a simultaneous measurement of the density profile. The results were compared to radiation hydrodynamics calculations which were in reasonable agreement with the data.

The targets consisted of triacrylate foam cylinders at a density of 50 mg/cc doped with 25% by weight of chlorine ($C_9H_3O_2Cl_5$). The foams were between 180 and 250 μm in length and 200 μm in diameter. The foam had a high degree of homogeneity with an average pore size diameter of approximately 1 μm. The cylinders were irradiated at one end by an intense soft x-ray pulse of 1.5 ns duration. The x-ray source was produced by a laser beam incident onto a burnthrough foil which consisted of 1500 Å of gold supported on a 1 μm substrate of parylene-N. The foil was positioned parallel to the face of the foam cylinder and separated from it by between 30 and 70 μm. The burnthrough foil was positioned behind a 200 μm aperture to ensure a clearly defined source size. Six beams of the VULCAN laser were focused in a cluster configuration (13 degree cone angle) to a 200 μm spot on the burnthrough foil producing x-ray irradiances up to 10^{13} W/cm^2. The soft x-ray flux and pulse shape were measured from the front and rear of the burnthrough foil by time resolved, frequency integrated, flat response x-ray diodes [9]. The induced ionization front was observed perpendicular to the axis of the cylindrical target. A flash radiograph was taken using point projection absorption spectroscopy. A source of x rays for the radiography was provided by a bismuth coated gold backlighter pin irradiated with 0.53 μm laser light with a pulse duration of 90 ps and focused with an $f/2.5$ lens. The pin was positioned typically 2.5 mm away from the foam target

 0031-9007/99/82(15)/3070(4)$15.00

resulting in an image magnification of approximately fifty times. The data were recorded, with a spectral resolution of 3 eV, using a spectrometer with a flat Rb-AP crystal ($2d = 26.12$ Å) and Kodak Industrex C-type film. The spectral range of the spectrometer was set to detect the absorption spectrum of chlorine due to transitions from the K shell to the $2p$ and $3p$ orbitals (i.e., 2.5–3.1 keV). The spectrometer was aligned to record the x rays passing through and around the foam allowing the absolute transmission of the foam to be obtained. Data were taken at different times, from between 1 and 2.5 ns after the start of the soft x-ray pulse, by varying the delay of the backlighting beam relative to the beams irradiating the burnthrough foil. The time resolution was determined by the length of the backlighter pulse, measured to be 90 ps. The spatial resolution was measured by radiographing alignment discs and grids and was found to be 10 μm in the propagation direction of the front.

The K-shell absorption data were compared to synthetic spectra generated from a detailed model of the population in configurations of the chlorine charge states in the foam. Saha-Boltzmann statistics assuming local thermodynamic equilibrium (LTE) were used to calculate the relative populations in configurations of the chlorine charge states with a full K shell. The model included all permutations of L shell electrons, satellites in M and N shells, and detailed term structure. A synthetic transmission spectrum was then constructed from the calculated populations, measured density, known pathlength, and the input temperature. This model has been described elsewhere [8,10]. The assumption of LTE was verified by non-LTE collisional-radiative calculations using the GALAXY code [11]. The calculations showed that for all physically reasonable radiation fields emitted from the burnthrough foil [12], the chlorine ion distribution did not significantly depart from LTE. The material density was obtained from the ratio of the measured continuum transmission through the front to that of material ahead of the front. The change in continuum opacity with ionization through the front was calculated using the opacity code IMP [13]. The adjustment to the density due to continuum opacity changes was up to 15%.

1D and 2D simulations were performed using the Lagrangian radiation hydrodynamics code, NYM [14]. The hydrocode included inverse bremsstrahlung and resonance absorption [15], flux limited thermal conduction with a flux limiter of 0.05 [15], multigroup opacities calculated from the IMP code, radiation transport using the Implicit Monte-Carlo formalism [16], and tabulated equation of state data [17]. The flux measurements from the x-ray diodes were used in the code and the simulated density and temperature profiles, the ionization and shock front positions were compared to those inferred from the experimental data. In the simulations the flux was varied by up to 18% from the diode reading to match the position of the front. This variation was within the accuracy of the diode flux measurement. Simulations indicate volumetric preheating of the foam to approximately 2 eV by hard x rays from the gold. This is predicted to close the voids in the foam in the first few hundred picoseconds of the heating pulse, producing a continuous medium.

A typical example of a radiograph showing the absorption lines of the chlorine dopant in the foam and the formation of a shock can be seen in Fig. 1. The x-ray flux on the foam target was 8×10^{12} W/cm^2 and the probing time was 1.8 ns. Region 1 is the shadow of a wire, 80 μm in diameter, which shields the spectrograph from seeing the emission from the burnthrough foil situated behind the wire. This shield wire also provides a means of discriminating the time integrated foam self-emission from backlighter emission. The emission line at a slightly lower frequency than the $1s$-$2p$ absorption lines is the

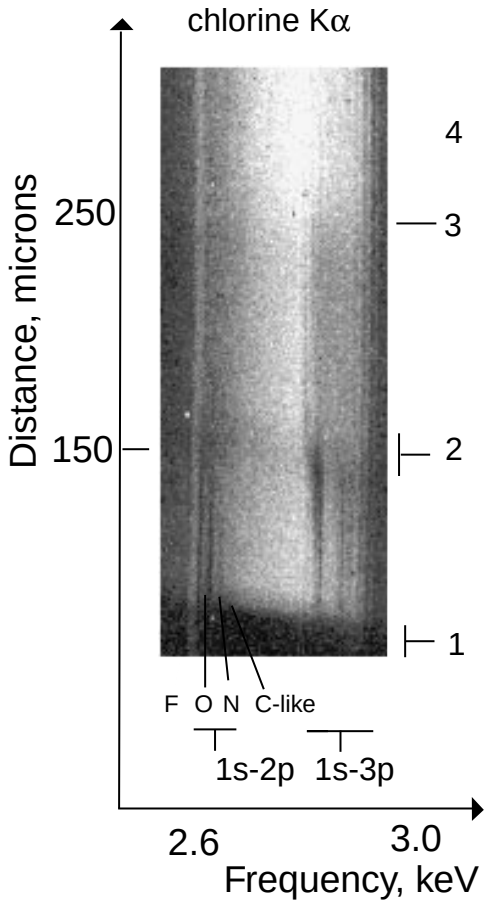

FIG. 1. A radiograph taken at the transition from supersonic to subsonic propagation. Region 1 is the shadow of a wire to block the spectrograph from emission from the burnthrough foil. Above region 1 the absorption lines of the chlorine doped into the foam can be seen due to transitions from $1s$ orbitals to $2p$ orbitals in each of the ion stages present in the foam with a $2p$ vacancy and due to transitions from $1s$ orbitals to $3p$ orbitals for all ion stages present in the foam. Region 2 shows the extent of the weak shock associated with the ionization front. The point marked 3 is the end of the foam. Region 4 is the unattenuated backlighter spectrum.

K_α fluorescence from the chlorine in the foam. This is produced by the component of radiation field from the burnthrough foil at frequencies above the cold chlorine K edge. In the radiograph above region 1 the absorption lines of the chlorine dopant can be clearly seen with both absorption from the $1s$ to the $2p$ orbital and the $1s$ to the $3p$ orbital recorded. Region 2 shows the extent of a weak shock associated with the ionization front. The point marked 3 is the end of the foam and region 4 is the unattenuated backlighter spectrum. Line scans of the absorption spectra were taken and compared to simulated spectra. The density inferred from the measured transmission was used in the atomic physics model, along with the known path length and the temperature then inferred by iterating the temperature in the model until the best match to the experimental absorption spectrum was obtained. Further iterations on the density and temperature were carried out to take into account the change in continuum opacity with ionization. A number of radiographs were taken of supersonically propagating fronts and these results used to select the flux and backlighter delay to study the ionization front as its velocity decreased. Figure 2 shows the temperature (a) and density (b) profiles inferred from a radiograph taken at a delay of 1.6 ns. Conditions in the front approach those at the boundary of the supersonic/subsonic transition as defined in Ref. [6]. The markers with error bars are the experiment, the solid lines are the 2D NYM predictions. Two curves of the NYM predictions are shown 100 ps apart to illustrate the degree of blurring due to the duration of the backlighter pulse. The calculated profiles were convolved with the measured spatial resolution. Temperature and density profiles in a target with a similar x-ray drive (8.8×10^{12} W/cm^2), inferred from a radiograph taken at a backlighter delay of 1.8 ns, are shown in Figs. 3a and 3b. Compared with Fig. 2 the result of Fig. 3 shows the ionization front has advanced approximately 20 μm, the temperature has fallen about 10 eV, and the density perturbation has increased to a peak value of just over twice the initial foam density. A slight change in the relative positions of the temperature profile and density profile in Figs. 2 and 3 shows the ionization front is gradually being overtaken by the density perturbation. The conditions in the ionization front shown in Fig. 3 are such the front has crossed the boundary of supersonic-subsonic propagation as defined by Ref. [6]. The separation of the ionization front and the density perturbation is more marked in Figs. 4a and 4b. In this case the x-ray flux driving the front was reduced relative to the results of Figs. 2 and 3 to 4×10^{12} W/cm^2 and the backlighter delay was increased

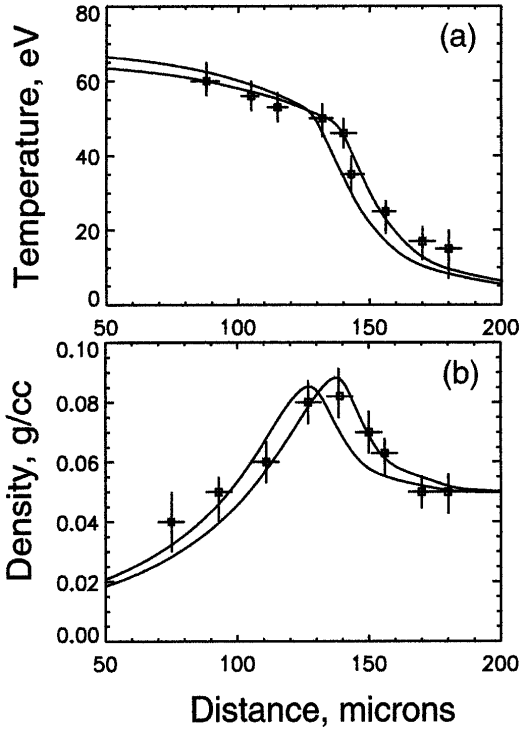

FIG. 2. The temperature profile (a) and density profile (b) inferred from a radiograph taken at a backlighter delay of 1.6 ns with an incident flux of 8×10^{12} W/cm^2. The solid curves are the NYM simulation, the markers with error bars are the experiment. The two curves from simulation are 100 ps apart and have been convolved with the measured spatial resolution. The ionization front is at the limit of supersonic propagation as defined by Hatchett [6].

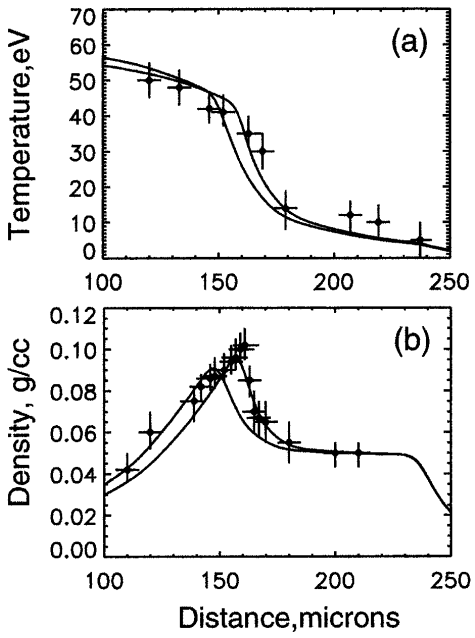

FIG. 3. The temperature profile (a) and density profile (b) inferred at 1.8 ns backlighter delay with an incident flux of 8.8×10^{12} W/cm^2. Markers with error bars are the experimental points and the solid lines are 2D NYM simulation predictions of the temperature and density profiles through the foam target. Two simulations are shown 100 ps apart to show the extent of motional blurring during the backlighter pulse. The calculation was convolved with the measured spatial resolution.

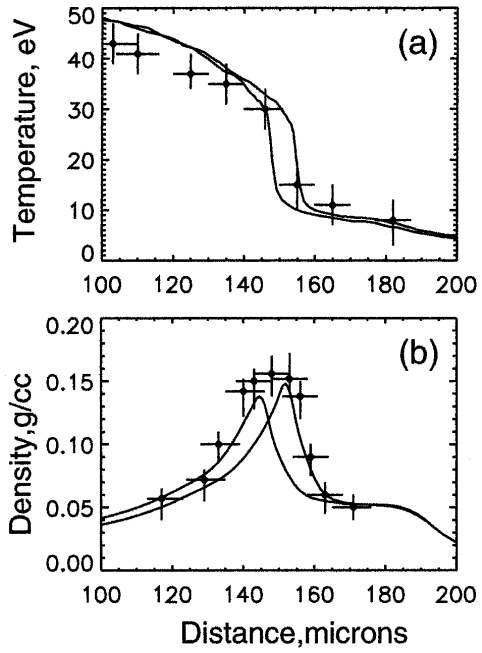

FIG. 4. The temperature profile (a) and the density profile (b) inferred from a radiograph taken at 1.9 ns backlighter delay. The flux was reduced relative to the data of the previous figures to 4×10^{12} W/cm^2. The density ratio has increased to over 3 and there is a separation of the shock and ionization front. The two simulations are 100 ps apart and have been convolved with the measured spatial resolution.

to 1.9 ns. The curves in Fig. 4 show an increase in the density ratio of the shock to over three times the initial density, a decrease of approximately 20 eV in the electron temperature, compared to Fig. 2a, and an increase in the separation of the temperature front and the peak of the density perturbation compared with the data shown in Figs. 2 and 3. In the result shown in Fig. 4 the ionization front is preceded by an ablatively driven shock. Ultimately conditions in the front should reach a strong shock condition with a density ratio of four in an ablatively driven shock. However, for the dimension of these foam targets, shock break out and rarefaction mean that this does not occur.

The positional error bars shown in the results are due to uncertainty in the position of the end of the foam and the width of the lineout scans taken through the data. The density errors are due to uncertainties in fog subtraction. The error in temperature is the temperature change needed to observe an appreciable difference between simulated and experimental absorption spectra.

In summary, the temperature and density distributions of ionization fronts propagating in a low density foam target have been measured in detail. For the first time the transient behavior of ionization fronts in the change from supersonic to subsonic propagation has been observed. The approximate analytical model of Hatchett [6] was used to define the boundary of supersonic propagation with a limit of two in the density ratio of shocked material behind a supersonically propagating ionization front before transition to subsonic ionization front propagation. The change from supersonic propagation was measured to occur at a density perturbation of 0.1 g/cm^3 at a time of 1.8 ± 0.1 ns for a drive flux of 8×10^{12} W/cm^2. The data have been compared to predictions of a 2D radiation hydrodynamics code which reproduced the measured behavior reasonably well, showing a smooth transition from supersonic to subsonic propagation. The detailed temperature and density profiles obtained from radiography are also in reasonable agreement with the NYM simulations.

We are grateful to the laser and target preparation staff at the Rutherford Appleton Laboratory for support during the experiments. We also thank C. Smith, Peter Graham, John Edwards, and Mike Dunne for their advice and useful discussions on the NYM code. This work was funded jointly by the SERC and MoD.

[1] D. Mihalas and B. W. Mihalas, *Foundations of Radiation Hydrodynamics* (Oxford University Press, New York, 1984).
[2] J. Lindl, Phys. Plasmas **2**, 3933 (1995).
[3] T. Afshar-rad *et al.*, Phys. Rev. Lett. **73**, 74 (1994).
[4] R. Sigel *et al.*, Phys. Rev. Lett. **65**, 587 (1990).
[5] W. I. Axford, Philos. Trans. R. Soc. London A **253**, 301 (1961).
[6] S. P. Hatchett, LLNL Report No. UCRL-53607, 1983.
[7] C. L. S. Lewis and J. McGlinchey, Opt. Commun. **53**, 179 (1985).
[8] D. J. Hoarty *et al.*, Phys. Rev. Lett. **78**, 3322 (1997).
[9] H. N. Kornblum and V. W. Slivinsky, Rev. Sci. Instrum. **49**, 1204 (1978).
[10] D. J. Hoarty, Ph.D. thesis, University of London, 1997.
[11] S. J. Rose, J. Quant. Spectrosc. Radiat. Transfer **54**, 333 (1995).
[12] D. R. Kania *et al.*, Phys. Rev. A **46**, 7853 (1992), and references therein; P. D. Roberts *et al.*, J. Quant. Spectrosc. Radiat. Transfer **51**, 19 (1994).
[13] S. J. Rose, J. Phys. B **25**, 1667 (1992).
[14] P. D. Roberts, AWE Report, 1980 (unpublished); P. D. Roberts *et al.*, J. Phys. D **13**, 1957 (1980).
[15] *Laser Plasma Interactions*, edited by R. A. Cairns and J. J. Sanderson (SUSSP, Edinburgh, 1979).
[16] J. A. Fleck and J. D. Cummings, J. Comput. Phys. **8**, 313 (1971).
[17] K. S. Holian, *T-4 Handbook of Material Properties Data Bases* (LANL, Los Alamos, New Mexico, 1984), Vol. 1c [EOS LA-10160-MS].